Effects of tropical cyclone paths and shelf bathymetry on inducement of severe storm surges in the Gulf of Thailand

Saifhon Tomkratoke[1], Sirod Sirisup[1]*

[1] Data-Driven Simulation and Systems Research Team, National Electronics and Computer Technology Center, Pathumthani 12120, Thailand

Abstract

The influences of tropical cyclone paths and shelf bathymetry on the inducement of extreme sea levels in a regional bay are investigated. A finite volume coastal ocean model (FVCOM) has been configured for the Gulf of Thailand-Sunda Shelf. A parametric wind model is used to drive the FVCOM. The contributions of the tropical cyclone characteristics are determined through a scenario-based study. Validation based on a historical extreme sea level event shows that the model can resolve the oscillation mechanism well. The intensification of severe storm surges in the region highly depends on four factors including phase propagation of the storm surge wave determined by the landfall position, funnel effect caused by locality of the coastline, and shelf bathymetry determined by the state of mean sea level and coastline crossing angle of the storm path. The coexistence of these factors can cause particular regions e.g. the Surat Thani Bay, inner Gulf of Thailand and Ca Mau Peninsular to experience a larger surge magnitude. These areas are found to be highly related to monsoon troughs that develop during the onset and early northeastern monsoon season (October–November).

Key words: storm surge, extreme sea level, shelf bathymetry, Gulf of Thailand.

---

1 Introduction

The threat of extreme sea level from storm surges to the South Asia and Southeast Asia has become an alarming issue since several disastrous events emerged in recent decades, e.g., in Bengal Bay (Cyclone BOB 01, 1991), the Andaman Sea (Cyclone Nargis, 2008) and the West Pacific (Super Typhoon Haiyan, 2013). In South Asia (SA), a six-meter storm surge induced by Cyclone BOB 01 submerged islands and devastated low-lying areas surrounding the Meghna Estuary of Bangladesh causing more than a hundred thousand casualties and leaving 10 million homeless. This colossal loss of life during the 1991 cyclone season was due to the widespread nature of the surges. As-Salek (1998) stated that the number of deaths caused by the BOB 01 storm surge accounted for more than 95% of the total lives lost in the event. In the upper Andaman Sea, adjacent to the Bengal Bay, Cyclone Nargis completely ruined Myanmar with more than a hundred thousand casualties together with the catastrophic destruction of properties and ecological systems. The level of surging water induced by that system was approximately six meters above the shoreline elevation. Records of the aforementioned storms indicate that one of the most critical issues that significantly contributes to losses is the denial of warning information together with storm underestimation by the prediction system. Storm underestimation also contributes to ineffective storm surge evacuation. A paradigm shift is needed to enable improvements in prediction and perception of surge-related disasters in SA. This shift has not significantly occurred due to limitations of the background conditions in conjunction with the relatively short period of archived tropical cyclone surge data.

For the Gulf of Thailand and the Sunda Shelf (GOT-SS), which

is representative of Southeast Asia (SEA), the recent period of severe storm surges extends back 50 years, in which only three surge events have been recorded: Typhoon Harriet (1966), Typhoon Gay (1988) and Tropical Typhoon Linda (1997). The time span of these events covers a few decades under the recent climate but the shelf emerged from the last glacial period. Hence, in assessing the vulnerability of the GOT-SS, we may instead need to rely on a relatively long period of evidence and a thorough understanding of storm surge mechanisms. From geologic evidence, the washover fans in two low-energy settings on the Gulf of Thailand (GOT) coast reveal that up to 19 typhoons struck the Thai Coast within the last 8 000 years (Williams et al., 2016). The prehistoric typhoons in the GOT are also evident by coastal deposit materials such as carbonate boulders, which have been discovered on Ko Larn Island near the head of the GOT (Terry et al., 2015). From this evidence, the derived sea current magnitude required to lift such carbonate boulders is in the range of 4.7 m/s and 7.1 m/s. This recent work can serve as reliable evidence of a historical severe storm surge to the coastal community. Hence, the belief that we are entirely safe from storm surge hazards can now be discarded based on this new evidence. Since the end of the 2nd millennium, catastrophic storm surge events in SEA did not occur, and damages from surges prior to 2013 were not severe. This made the 2013 strike by Super Typhoon Haiyan in the Philippines particularly surprising. The magnitude of the Haiyan storm surge had never been previously reported since the related agencies began documentation of storm surge disaster events, hence, the warning information was rejected, resulting in massive losses.

Regarding hydrodynamic mechanisms, for SEA, the surge

---

*Corresponding author, E-mail: sirod.sirisup@nectec.or.th

mechanism induced by Super Typhoon Haiyan (2013) as well as other legendary cases has not been thoroughly investigated yet. However, a few works focus on recreating the event and providing a surge map. In another region, the Bay of Bengal, vital information on the mechanism of widespread surges has been revealed by As-Salek (1998), Flather (1994), and Debsarma (2009). Their results indicate that the combination of coastal trapping and the funnel effect can result in a widespread storm surge. Recently, the nature of surge–tide interactions in the Bay of Bengal has been investigated (Hussain and Tajima, 2017). For the coastal area in the SEA region, this issue has not yet been further investigated or affirmed. The variability in climate conditions due to climate change may result in considerable uncertainty in predicting a tropical cyclone (TC) in any region, especially in the SEA region. Hence, the awareness of storm surge impact remains vital and necessary for us.

Throughout the coastal communities of the world, there have been significant efforts to improve both prediction systems and the efficiency of mitigation plans to handle storm surge issues. In doing so, an insight into storm surge dynamics for each particular basin is vital and customarily needed. In the current study, we mainly focus on the GOT. In the past few years, investigations of cyclonic wind-induced storm surges that involve model development and validation are found in Kanbua et al. (2005), Phaksopa and Sojisuporn (2006) and Aschariyaphotha et al. (2011). For determination of surge mechanisms, Vongvisessomjai (2007) has reported that fetch length can be an important factor in the production of a massive surge. Recently, Sirisup and Kitamoto (2012) presented a normal mode structure of the GOT. The modes were used to reproduce characteristics of the storm surge induced by TC Linda in 1997 with reasonable accuracy. Later, Tomkratoke et al. (2015) confirmed that modal structures and interactions between the disturbance system and propagating surge waves in the gulf can induce large positive surges.

However, to the best of our knowledge, a comprehensive mechanism of storm surge dynamics in coastal bay systems including the influence of cyclonic wind characteristics, the funnel effect and mean sea level, has not been fully investigated. Especially for the GOT, a comprehensive mechanism of storm surges has not yet been determined, which reduces the accuracy of storm surge predictions and risk assessment systems for the region. The current study aims to address these issues. The investigations are performed with numerical experiments using the finite-volume coastal ocean model (FVCOM) (Chen et al., 2003) together with atmospheric perturbation forcing data based on a parametric wind model (Holland, 1980).

The remainder of the paper is organized as follows: Section 2 presents the methodology, the results and discussion are presented in Section 3, and our conclusions are in Section 4.

2 Methodology

2.1 *Study area and model configurations*

2.1.1 *Study area*

The location, configuration of coastlines and seabed topography of the GOT are shown in Fig. 1a. We refer to the GOT as a sub-basin of the South China Sea (SCS) known as the Sunda Shelf (SS). The GOT includes sea territories of Thailand, Cambodia, Vietnam, Malaysia and China. Its location is from 1.33ºN to 14.00ºN and 99.00ºE to 112.00ºE. The GOT is a broad and shallow sea with 52.0 m average depth. A much deeper sea with 2 000.0 m average depth (the SCS) connects to the eastern entrance of the GOT
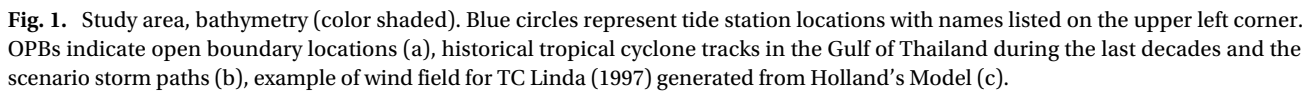
while the Kalimantan Strait-Java Sea connects to the southern entrance. A unique feature of this region is that overall, it can be addressed as either a wide continental shelf or a wide shallow coastal bay.

The uniqueness of oceanography is a result of such geological settings. A strong standing wave oscillator with a moderate energy dissipation rate (Tomkratoke et al., 2015) is one of the unique natures of the GOT. This characteristic causes the largest amplitude of the major tide (K_1) is merely 0.67 m (Zu et al., 2008) and is only found at the headend of the region (the inner GOT). The tide is associated with modest current magnitude of approximately 0.40 m/s (Saramul, 2017). Besides, the spatial dynamic of semi-diurnal tides are mainly influenced by both of basin resonance (Tomkratoke et al., 2015). The characteristic of M_2 tide near the Ca Mau Peninsular in Vietnam, Kuching-Samarahan-Betong in Sarawak, Malaysia and as well the inner GOT are in good agreement with such characteristic. Thus, tidal ranges in those regions are relatively high which also suggests the important coastal shelf morphology. The significance of tide-surge interaction in the regions has not yet been completely determined in the present. However, in overall, it tends to show a less influence on amplification of the storm surge as investigated by Tomkratoke et al. (2015). In contrary, the influence of topographic and bathymetric factors tend to be higher. To determine factors producing severe storm surge in the GOT, influences of tides are thus suppressed in the current study.

For calculations in a Cartesian coordinate system, map projection of the study area and all spatial data are transformed to the Universal Transverse Mercator (UTM) coordinate system. For creating the computational domain, the study area is subdivided into 80 000 triangular grids. The grid resolutions of approximately 4 000 to 8 000 m are used for the shelf and deeper zones while the finer resolutions of approximately 300 to 1 000 m are applied in the coastal regions. For representing the geometric complexity of the study area well, high fidelity bathymetric data with a resolution of 30 s from GEBCO (General Bathymetric Chart of the Oceans) is used (IOC-IHO, 2003). The computational domain covers an area of approximately 880 000 km² (Fig. 1a).

2.1.2 *Model configurations*

The ocean hydrodynamic model used in this study, FVCOM, was developed originally by Chen et al. (2003) and upgraded by the University of Massachusetts-Dartmouth/Woods Hole Oceanographic Institution (UMASS-D/WHOI) model development team (Chen et al., 2006). The advantages of FVCOM for coastal and ocean applications include the model's use of an unstructured triangular mesh to subdivide the horizontal computational domain. In the vertical computational domain, the σ coordinate transformation is applied to obtain a smooth representation of the irregular bottom topography. Thus, the geometric complexity of the shoreline and seabed is preserved. Importantly, the primitive equations of the model can be switched to Cartesian or spherical coordinate systems. Further, optional turbulence closure schemes, e.g., Smagorinsky, modified Mellor and Yamada level 2.5 (MY-2.5), and k-ε turbulence closure schemes, are provided for a mathematically closed form of the primitive equations. FVCOM solves the underlying equations by using a flux calculation integrated over each model grid control volume with a mode-splitting method for external and internal mode time steps to accommodate faster and slower barotropic and baroclinic responses. These model characteristics allow accurate and efficient resolution of the underlying physical mechanism associated with the resonance of long waves and other wave-related

Fig. 1. Study area, bathymetry (color shaded). Blue circles represent tide station locations with names listed on the upper left corner. OPBs indicate open boundary locations (a), historical tropical cyclone tracks in the Gulf of Thailand during the last decades and the scenario storm paths (b), example of wind field for TC Linda (1997) generated from Holland's Model (c).

hydrodynamic mechanisms. A more detailed description of the FVCOM code can be found in Chen et al. (2003).

Characterization of extreme sea levels only generated by a cyclonic disturbance is the primary objective of the current study. Hence, other contributions such as tides and seasonal mean sea levels are disregarded. The model configuration for this purpose is as follows: the radiative boundary type is applied at open boundaries of the domain (Fig. 1a), e.g., sea surface elevation is calculated using a gravity wave propagation speed, $\sqrt{gh}$, where h is the water depth; the parameter for the effect of the bottom drag coefficient is set to follow a log model with the lowest value of 0.004; the zero free surface water elevation and sea current velocities are the model initial conditions. The simulation will be performed within the time length of 120 h. To ensure that the model stability, the temporal resolution of 1 second is applied. The driving force is cyclonic disturbances generated by a parametric wind model, the details of which are described next.

2.1.3 *Driving force*

The interaction between cyclonic wind and the ocean creates wind stress on the sea surface that is controlled by the strength of the wind. This wind stress generates most of the tropical cyclone-induced surges (Kohno, 2007). Thus, the inverted barometer effect can be excluded. However, to accurately simulate the dynamic behavior of storm surges, appropriate TC wind data is ne-

cessary. Unfortunately, measurements are usually unavailable. Reanalysis climate data may be recommended as an alternative resource for storm surge studies. However, such data can indeed reconstruct well for ambient wind surrounding the TC cell but the wind speeds near the cyclone center are normally lower than actual values (Cavaleri and Sclavo, 2006; Signell et al., 2005). This limitation may significantly suppress reconstructing storm surge dynamic behaviors especially near TC landfall areas, particularly for small TCs. Although improving TC wind field from hindcast datasets is possible as proposed by Pan et al. (2016), however, using such data in scenarios based study related to the TC translation paths can be rather unsuitable. In the present study, because the effect of the TC paths on the development of storm surges is our primary objective, thus, a more suitable approach should be applied. To this end, a parametric wind model such as Holland's model (1980) can be used to provide tropical cyclone wind data. The results from this parametric wind model are used to drive the ocean hydrodynamic model. From Holland's model, the radial velocity (VR) distributed from the storm center can be expressed as:

$$\text{VR} = \sqrt{\frac{B\,(P_a - P_c)}{\rho}\left(\frac{\text{RMW}}{R}\right)^B \exp\left[-\left(\frac{\text{RMW}}{R}\right)^B\right] + \frac{R^2 f^2}{4}} - \frac{Rf}{2},$$

(1)

where P_a is the ambient pressure, P_c is the central pressure, B is the hurricane shape parameter which can be calculated from $B = 2 - \dfrac{P_c - 900}{160}$ but is only valid for $1 \leqslant B \leqslant 2.5$, RMW is the radius of maximum wind speed, R is the radial distance from the center of the storm, f is the Coriolis parameter, and ρ is the air density. To determine the Holland's model parameters, the tropical cyclone data from Digital Typhoon (Digital Typhoon, 2016) have been applied. An example wind field of the considered tropical cyclone event (Linda, 1997) generated by this model is presented in Fig. 1c.

To incorporate the wind field in the FVCOM, the surface wind stress must be calculated. The surface wind stress is computed as follows:

$$\left(\tau_{sx}, \tau_{sy}\right) = C_{ds}\rho_a\sqrt{W_x^2 + W_y^2}\left(W_x, W_y\right), \qquad (2)$$

where (W_x, W_y) are the x and y components of the wind velocity, and ρ_a is the air density. The sea surface drag coefficient, C_{ds}, depends on the wind speed, $W{=}\sqrt{W_x^2 + W_y^2}$, and takes the form of:

$$C_{ds} = \left\{ \begin{array}{ll} 1 \times 10^{-3}, & \text{for } W \leqslant 7 \text{ m/s} \\ (0.192\,3 + 0.115\,4W) \times 10^{-3}, & \text{for } 7 \leqslant W \leqslant 20 \text{ m/s} \\ 2.5 \times 10^{-3}, & \text{for } W \geqslant 20 \text{ m/s} \end{array} \right. \qquad (3)$$

2.2 *Scenario-based simulations*

2.2.1 *Storm paths*

According to the statistical data from Digital Typhoon (Digital Typhoon, 2016), it is known that the intensification of TCs in the Western Pacific is associated with the occurrence of monsoon troughs (MT). The close relationship between TC activity and MT location in this region was revealed by Wu et al. (2012) and Takahashi et al. (2015). Moreover, Lander (1996) stated that the average location of the monsoon trough in the area shows a seasonal response. This enables us to estimate the major characteristics of TCs under constrained climatic circulation. Guided by variation in the monsoon trough locations over the GOT-SS, the translation path of TCs may be estimated. The present study applies this path estimation approach to approximate four storm paths derived from dominant troughs over the GOT (Fig. 1b). As seen in Fig. 1b, the two upper paths (denoted by TC1_OSM and TC2_ENE) are representative of a monsoon trough that occurs during the onset and early northeastern monsoon season, i.e., October and November, respectively. The distance between these two paths is approximately 250 km.

In the context of storm surge hazards, effects of TCs developed by equatorward movement of MT have not yet explored in the GOT-SS, therefore, the other two paths such as TC3_MNE and TC4_LNE are included in the current study. The TC3_MNE path is associated with the period of mid northeastern monsoon (December) where the MT band normally passing over the end of Southern Thailand. The TC4_LNE path supports the scenarios that the MT band become predominated over Malaysia (January-February). These paths are shifted southward, 250 (TC3_MNE) and 500 (TC4_LNE) kilometers from the location of the TC2_ENE path, respectively. Additionally, the intensity of all the modeled storm is 37 m/s (category one on the Saffir-Simpson scale) with a translation speed of 21 km/h until landfall.

2.2.2 *Mean sea level conditions*

Theoretically, amplification of storm surges in shallow continental shelves is influenced by shelf bathymetry. This amplification occurs as the storm surge waves propagate in the decreasing shelf depths. This mechanism has been confirmed by Horsburgh and Wilson (2007) with their finding that a reduction in surge magnitude occurred at the moment of high water. Moreover, Rego and Li (2010) found that peak water levels were lower than expected for a landfall at high tide. Their results emphasize that large surges can be intensified more over shallow continental shelves than over deep continental shelves. These findings can be directly applied to the GOT-SS, however, an interesting question is how the scenario changes with sea level variability. To clarify this issue, we perform numerical experiments under different mean sea level conditions in which the mean sea level varies in the range of +2.0 to –2.0 m from the baseline. The interpretation of these results should be helpful to those concerned with how storm surges respond to sea level variability.

3 Results and discussion

3.1 *Model validation*

To ensure the hydrodynamic and tropical cyclone models used in the present study are accurate and the resulting insights on physical mechanisms are reasonable interpretations, a model validation needs to be performed. Here, the characteristics of extreme sea level caused by TC Linda (1997) are reproduced using the FVCOM (Fig. 2). These results are validated against the observation sea levels retrieved from the University of Hawaii Sea Level Center (uhslc.soest.hawaii.edu). Specifically, the recorded data for Koh Lak (Thailand), Vung Tau station (Vietnam) and two additional stations in Malaysia are selected for validation purposes and for completeness in interpreting the overall physical mechanism. The locations of these stations are presented in Fig. 1a. It is noted that the storm surge level at each station is a departure from the typical tide and seasonal water levels.

As shown in Fig. 2, the surge magnitude and fluctuation patterns of the storm surges are in good agreement with the observations. The current model captures the negative surge and positive surge of TC Linda (1997) in the GOT and the adjacent shelf with reasonable accuracy. However, the simulation tends to underestimate positive surges at the Koh Lak and Geting stations (Fig. 2, a and b). In Fig. 2, c and d, the observed sea water levels at the Vung Tau and Bintulu stations show significant effects of wind setup (rising period of the maximum surge level) and the model result produces good agreement with both the trends and fluctuation periods. Nevertheless, the overestimation of surge magnitude is obvious.

The difference between observed and modeled results at these two stations indicates that the use of a parametric wind model for simulating a storm surge dominated by wind setup needs more precise information on storm characteristics. Moreover, the amplification processes of storm surges in real situations can be far more complicated than this model's capability. These types of discrepancies are typically found with simulations near coastal bays where the amplification of long waves can be intensified by shallow water effects together with local bed friction; hence, simulation typically produces underestimation or overestimation when local seabed topography is treated as regional. Furthermore, compared with the earlier study by Phaksopa and Sojisuporn (2006), predictions by the current simulation are significantly improved based on the reproduction of the
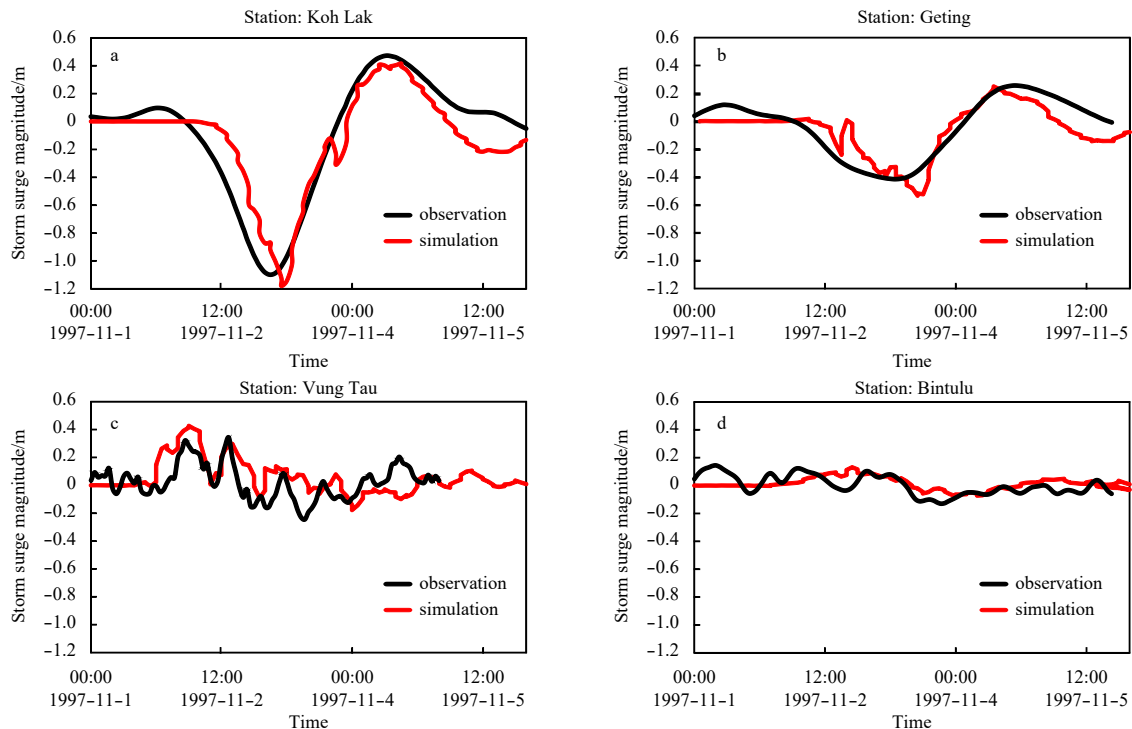
Fig. 2. Measured and simulated storm surge levels for each station: a. Koh Lak, Thailand; b. Geting, Malaysia; c. Vung Tau station Vietnam and d. Bintulu, Malaysia.

TC Linda (1997) storm surge. Therefore, based on the current simulation results, the underlying mechanism of the storm surge induced by TC Linda (1997) can now be accurately characterized. Further details are discussed next.

Undulation of the sea surface and circulation patterns during the passage of TC Linda (1997) over the GOT-SS are shown in Fig. 3. During the period of the negative surge (Figs 3a and b), the TC (with 50 kn intensity) is located approximately 450 km off the Surat Thani coast, Thailand. The system induces a large undulation of the sea surface with a negative surge covering the middle to upper north area of the gulf. The water current pattern induced by TC Linda (1997) is characterized by a large counterclockwise rotation flow cell located near the northern part of the gulf (Fig. 3a). Interacting with beaches and seabed topography, the structure of the rotating cell is better developed in a larger cell surrounded by stronger currents. This rotating flow also causes the water mass to move away from the GOT into the vicinity of the TC, thereby depressing the surge amplitude or the negative/ebb surge phase (Fig. 3b). The current study also shows that influence of the typhoon on the oceanic processes in the GOT even when the storm intensity weakens to a depression system. In contrast, during the period of the positive surge (Figs 3c and d), the rebounding water mass occurs 12 h after the tropical cyclone reaches the southern coast of Thailand (approximately 159 hours after 29/10/1997 00:00:00 UTC).

The characteristic mirrored N-shaped surge pattern (negative followed by positive) can be seen in Figs 2a and b. Conforming to the fundamental mode structure of the gulf (Sirisup and Kitamoto, 2012) in the period of approximately 58 h, the induced storm surge can properly fit into the gulf geometry and develop a single nodal band at the shelf entrance (Figs 3b and d). However, other contributions, especially wind setup and topographic amplification effects, have not yet been clarified. The importance of

such contributions can be seen at the Vung Tau and Bintulu stations. Note that the surge pattern at these stations shows abrupt changes in sea level instead of gradual changes such as in the mirrored N-shaped surge at the Koh Lak station (Fig. 2a). Hence, wind setup appears to be the dominant factor for this phenomenon. This issue will be investigated and confirmed in future work.

3.2 *Influence of the storm path*

A funnel effect is considered here because the triangular shape of the bay can confine the concentration of surge energy. This issue was pioneered by Proudman (1955) who stated that the convergence at coastlines could lead to surge amplification. Topographic influences on amplification of a surge in the GOT have never been accounted for in the development of a surge mitigation scheme. Overlooking this mechanism may reduce the efficiency of storm surge hazard management. In this section, the significance of topographic influences on storm surge amplification along the Thai coast is presented. The funnel effect can be seen as clusters of large positive surges located at the coastal convergences of Thailand, Cambodia and Vietnam (Figs 4a and b). However, surge height differences in each particular area are significantly related to the characteristics of the TC path and will be fully described next.

3.2.1 *TC1_OSM path*

In this scenario, the TC path crosses the Vietnam coast before making a second landfall in Prachuap Khiri Khan, Thailand (Fig. 4a). This track is almost the same as TC Linda's (1997). The path direction of TC1_OSM and TC Linda is nearly perpendicular to the western Thai coast. Long stretching beaches mostly characterize the landfall location in this scenario, and two convergent coastlines, the inner GOT and the Ban Don Bay, are situated above and below the landfall location, respectively. As the storm ap-
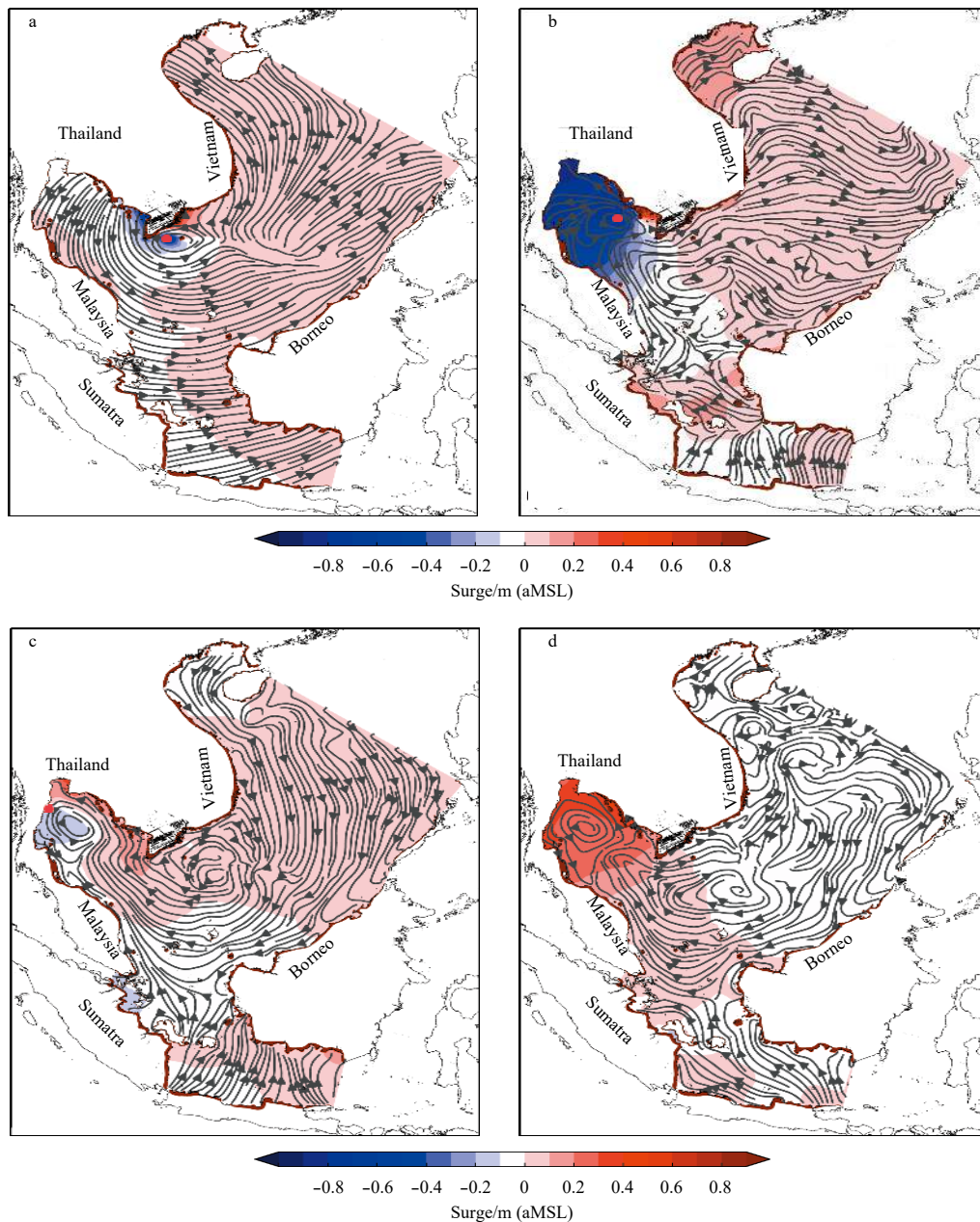
Fig. 3. Characteristics of sea surface and circulation during the passage of TC Linda (1997). The storm crossed the tip of Ca Mau (a) located approximately 450 km off Surat Thani, Thailand; negative surge (b); landfall (c); positive surge period (d) the storm moved inland.

proaches the coast, the wind front induces asymmetric sea levels at the landfall position (Fig. 5a, red and green curves). Figure 5 also presents surge levels from various mean sea level conditions. In this section, we mainly consider the storm surge result in relation to the baseline mean sea level. The results associated with other mean sea level conditions are interpreted in the next section.

In this scenario, the swelling sea level intensifies on the approaching wind front (AWF) yielding the largest surge on the western coast of the inner GOT. In contrast, the lowered sea level occurs on the retreating wind front (RWF). This is due to the water mass being pushed away from the coast into the sea resulting in a relatively low positive surge region near the landfall location. This asymmetric surge characteristic is found in all scenarios. The funnel effect, where the wind-driven water mass experi-

ences convergence at the coastlines, is also significant here. More precisely, the confined surge contour appears in particular areas of the Thai coast, i.e., Phetchaburi to Samut Prakan and Laem Ngop Bay. Similar confined surge contours are also found in Kampot, Cambodia and western Ca Mau, Vietnam. Furthermore, the mirrored N-shaped surge is also found in fluctuation of storm surge at the landfall location (Fig. 5). It suggests that seiche oscillation is inductive mechanism for development of the storm surge. The maximum positive surge should be explained as the coincidence of rebounding water mass from the nearby region and wind setup.

3.2.2 *TC2_ENE path*

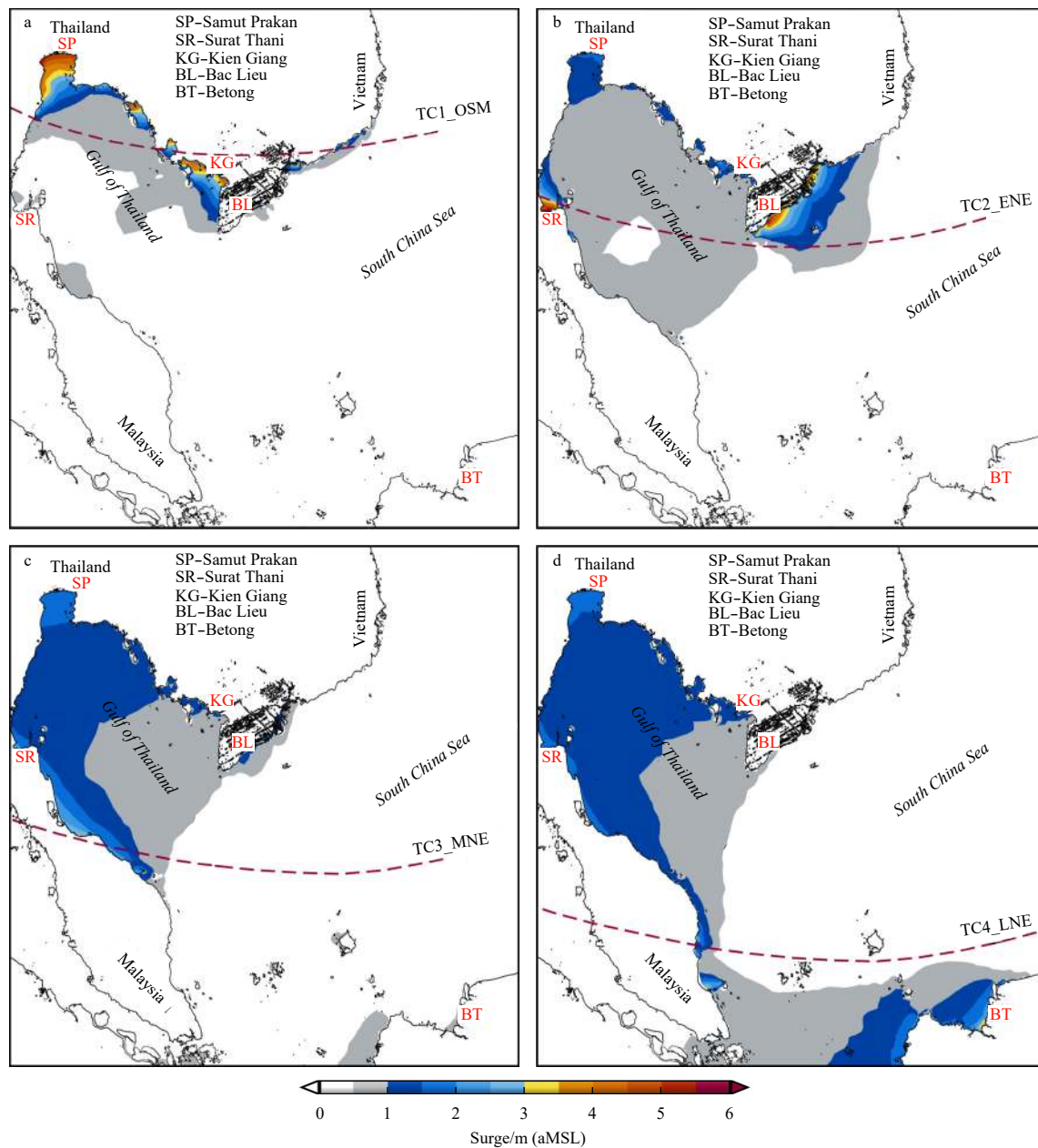In this scenario, the TC path makes landfall in southern Thail-

Fig. 4. Maximum storm surge magnitudes above mean sea level (aMSL) for the hypothetical TC paths. SP, SR, KG, BL and BT represent the probe locations with names listed on the upper edge.

and. The orientation of the coast relative to the storm direction is similar to that in the previous scenario but with a shorter distance to the southern coastal convergence (Ban Don Bay, Surat Thani) (Fig. 4b). The predominance of the funnel effect is clearly seen. In this scenario, larger and smaller surge magnitudes are observed inside the bay and the inner GOT, respectively. In the area with high amplification, Ban Don Bay, water-trapping morphologic structures cause the wind-driven water mass in the retreating wind front to be trapped. As a result, more water mass accumulates inside the bay (Fig. 4b). For this path, the fluctuation of the storm surge at the landfall position is also characterized by asymmetric sea level (Fig. 5b, red and green curves). The maximum storm surge level (approximately 2 meters) seem to be closed to that of the upper path (TC1_OSM), however, the duration of the positive period is longer. Indeed, this finding is associ-

ated with the path length to support the effective times for interactive process between the TC and sea body. Suggested by Figs 5a and 5b, the mechanism explaining development of the positive surge is the same as that of the TC1_OSM path.

Interestingly, the amplification of surge magnitude also appears at a weaker coastal convergence on the eastern coast of Ca Mau (Bac Lieu), Vietnam (Fig. 4b). Moreover, the surge level is relatively high (Fig. 7c). To explain the governed mechanism, another factor, coastline crossing angle, is considered. In this case, although the TC does not cross the Vietnamese coast directly, it is quite close. The translation path of the TC is approximately 40 degrees (measured from the storm path to the coastline in the counterclockwise direction) to the eastern coast of Ca Mau. Hence, the crossing angle is relatively small compared to those of the other tracks. This may be the marginal angle for supporting
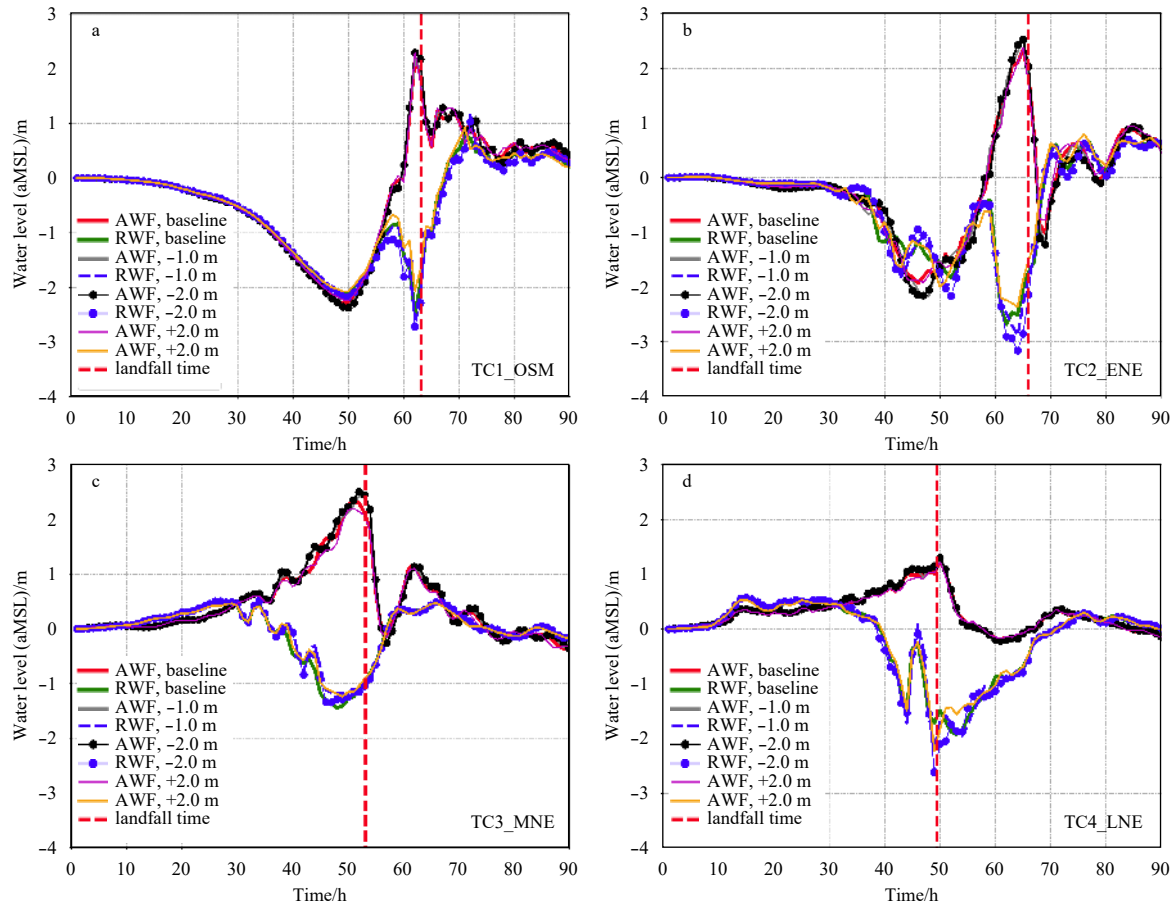
Fig. 5. Asymmetric sea levels occurred near landfall locations. Red and blue dash lines represent approaching and the retreating wind front (AWF and RWF). Red dash line indicates the landfall time for each scenario.

effective wind-driven water mass (induced by the approaching wind front) build up at the coast. According to As-Salek (1998) and Jelesnianski (1965), cyclones with a small angle of crossing can produce widespread surges in the coastal area while a larger angle can reduce the energy input and the velocity of the cyclone's translation along the coast.

3.2.3 *TC3_MNE path*

In this scenario, the approaching TC also makes landfall near a weaker coastal convergence (Pattani Bay) (Fig. 4c). The crossing angle of the path is larger than those in other scenarios (approximately 140 degrees measured from the TC path to the Songkla-Pattani coastline). The storm surges at the landfall location of this path are shown in Fig. 5c. In comparison, the maximum positive surge influenced by the characteristic of the path and coastal topography is slightly different from those of the two upper paths. On the contrary, the period of high surge level (approximately 2 meters) is significantly longer. Unlike TC1_OSM and TC2_ENE paths, the development of the maximum positive surge mainly shows the hydrodynamic response proportional to the wind strength. This confirms the effects of wind setup as described previously in the validation section. Interestingly, the reduction of ebb surge shows a lesser contribution of the RWF than the other cases (Fig. 5). We speculate that the convex-shaped coastline (Terengganu coastline in Malaysia) may reduce the strength of retreating sea current to push the water mass away from the coast leading to a lower ebb surge magnitude at the landfall location although the wind strength is similar to the oth-

er scenarios.

However, a widespread surge in the inner GOT still occurs with modest magnitudes. This result raises the question: when the contributions of topographic mechanisms become less pronounced, what other significant mechanisms can help explain the result characteristics adequately? Following the distribution of sea levels (Fig. 4c) from this TC, the storm surge indeed propagates along the North-South axis of the gulf instead of following along the coastline as an edge wave would. This is similar to the mechanism that describes the TC Linda (1997) surge presented earlier. Indeed, this appears to be governed by a seiche oscillation.

3.2.4 *TC4_LNE path*

Sensitivity to the funnel effect and crossing angle is observed again in this scenario (Fig. 4d). The first factor is intensified most in the Samarahan-Betong region of Sarawak, Malaysia because of its triangular-shaped bay. A cluster of large storm surges is found in the inner bay.

The comparison of the storm surge from different landfall locations dominated by the AWF effect is beneficial for going insight the latter factor. We mention on the development of the storm surge along the eastern coast of Ca Mau in Vietnam again. It is noted that the approaching TC and the coastline of such region make a small crossing angle of 40º. This lead to a more effectiveness of the AWF to produce large positive surge level. On the contrary, the TC4_LNE makes landfall at the southern Terengganu coastline and is associated with 100º of the crossing angle. There-

fore, at the landfall location, significant decrement of the maximum positive surge by increment of the crossing angle is instead obtained (Fig. 5d).

Though the path of TC3_MNE and TC4_LNE is parallel, their crossing angle associated with the AWF can be different by the coastline configuration. Therefore, the former is the largest crossing angle scenarios as it approaching the southern Thailand as mentioned earlier. Indeed, significantly smaller crossing angle characterizes the characteristic of the latter. The effect of crossing angle still valid for explaining development of the max positive surge for them, however, the contamination from the coastal convergence effect could also explain the different of the amplification.

For these TCs, the mechanisms governing the asymmetric sea level are mainly the effect of AWF and RWF. However, it is seen that the ebb surge (RWF contribution) at the landfall location for the TC4_LNE tends to be more pronounced. On speculating the mechanism behind this phenomenon, the lesser effect of the coastline shape to obstruct the RWF contribution should be addressed. Furthermore, as compared to the two upper paths, this scenario tends to increase the widespread surge over the GOT but with modest magnitude. Thus, under this scenario, the GOT coastal impacts such as damaging surge height may be reduced.

3.3 *Phase propagation*

In Fig. 6, the characteristics of storm surges near the inner GOT (Samut Prakan) are presented as induced by the hypothetic-

al TC scenarios. All the hypothetical TC paths make landfall coincidently with a positive surge phase. However, the induced surges tend to increase as the landfall and peak times become closed. This behavior coincides with the interactions of the storm wind for propagating surge waves. Further, such processes together with topographic influences can potentially lead to high positive surge magnitudes. Note that the baseline is only interpreted in this section.

According to storm surge characteristic (Fig. 6) and the position of the inner GOT location (Fig. 1), it is seen that the closer paths (TC1_OSM and TC2_ENE) induce the signature of mirrored N-shaped surge. On the contrary, the farther paths (TC3_MNE and TC4_LNE) mostly show a typical positive surge or flood surge. Besides, an increase/decrease in surge magnitude is found in the scenarios where TC paths are closer/farther from the inner GOT coast. However, as seen in Figs 6b and c, one of the mechanisms found here is that for a TC being far from the inner GOT coast such as TC3_MNE can produce a surge that is as high as surges from that of the closer one (TC2_ENE, for example). This result can be explained by the interaction of the TC with the negative surge phase such found in the TC2_ENE case. In contrast, a higher surge can occur as the advancing TC coincides with positive surges as found in the TC3_MNE case.

According to Tomkratoke et al. (2015), a TC that is coincident with a positive surge period (e.g. a time period that surge level is above mean sea level) can enhance the storm surge response magnitude. In contrast, lower enhancement occurs during a neg-
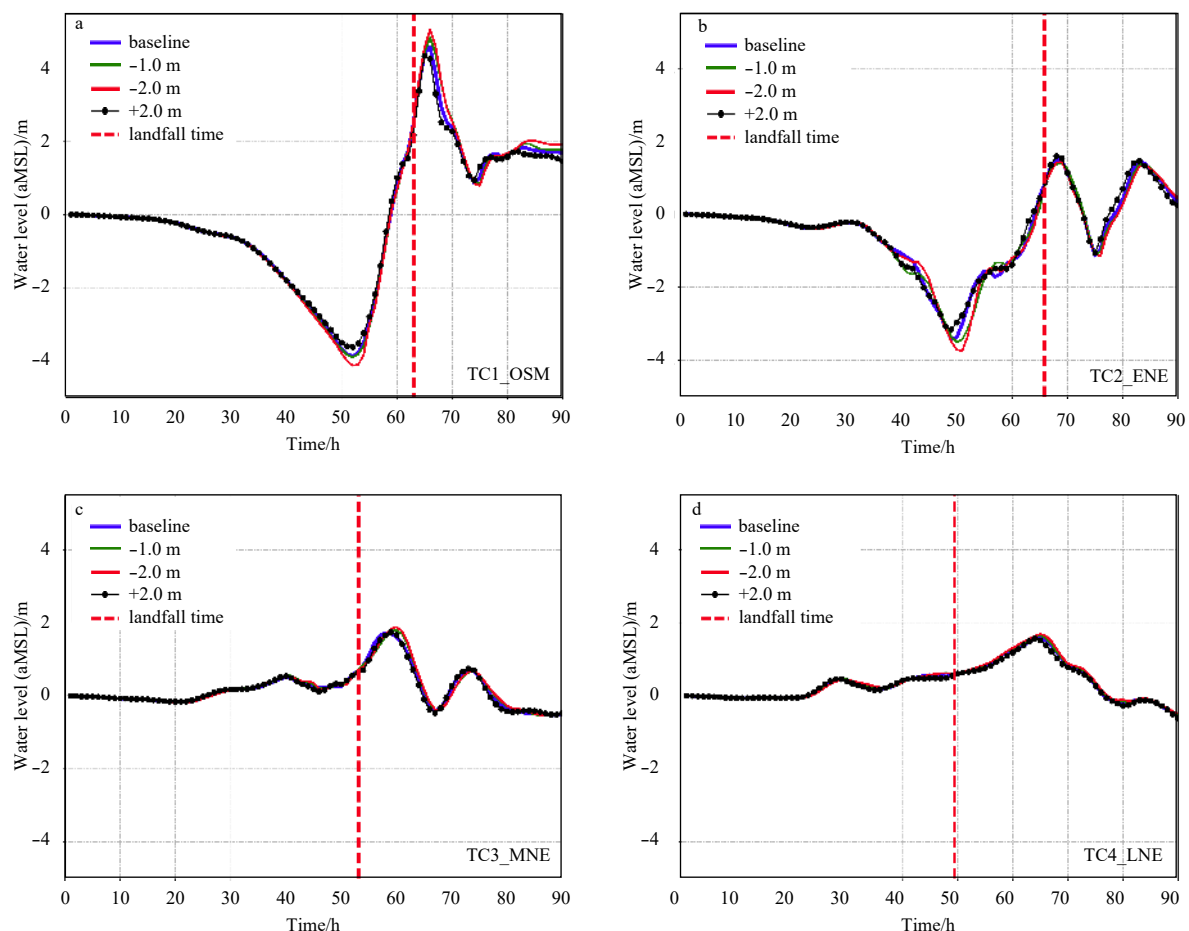

Fig. 6. Variation of sea levels in the inner GOT (Samut Prakan) influenced by hypothetical tropical cyclones and mean sea level (MSL) conditions. Dash line indicates the TCs landfall time for each scenario.

ative surge period (e.g. a time period that surge level is below mean sea level) even when the storm intensity increases. The behavior of TCs coincident with positive surge periods may support the development of a severe surge in the GOT-SS. This can help in assessments of rising coastal sea levels in the inner GOT during remote disturbances. Precise determination of landfall location and phase propagation of storm surge waves would significantly benefit efforts in preparation and prediction of storm surges in this region.

3.4 *Effects of mean sea level conditions*

In this section, the influence of shelf bathymetry on storm surge responses in the GOT-SS is presented. The impacts of storm paths are retained in the simulations, and various scenarios of mean sea level are applied to investigate their effects. To determine the magnitude of mean sea level variability, various contributing sources including tides, seasonal variation and projected sea level are considered. These sources can cause fluctuation in mean sea level in the gulf with amplitudes of 1.5, 0.2 and 0.3 m, respectively. Hence, a range of variability of 2.0 m above the present mean sea level can be reasonably used. Testing of the sensitivity of mean sea level in a real domain using hypothetical TC paths base on the variation of MT, our simulation should reveal the surge-sea level variation interaction for storm surges in this region and address concerns of storm surge sea level-dependent problems for the affected communities.

Overall, the behaviors found in the previous section persist

but significant effects of shelf bathymetry are observed. It is found that the storm surge magnitude tends to increase during low water conditions. In contrast, surge response is less during high water conditions. Consequently, the sensitivity of storm surge to the shelf bathymetry is higher nearshore than offshore region. For this reason, specific coastal regions, i.e., the inner GOT: Samut Prakan and Surat Thani, Kien Giang and Bac Lie, Vietnam and Betong, Malaysia, can potentially produce high surge magnitudes. Furthermore, the surge behavior in these regions tends to relate to the funnel effect. As a result, the storm surge in the nearshore areas can be intensified by shelf bathymetry and funnel effects while surges in the offshore areas may be significantly influenced by seiche oscillation. Next, more details on the issue are presented.

3.4.1 *Seiche mode*

In Fig. 5–7, a time series of storm surges obtained in the GOT-SS are interpreted. The overall mechanism and unique characteristic of storm surge propagation associated with storm paths for the baseline case have been discussed in Section 3.2 and 3.3. In this section, we mainly focus on the influence of mean sea level on the seiche mode of the storm surges.

It is found that time to peak for storm surges or seiches is delayed or accelerated as the mean sea levels vary. The case representing this result is mainly associated with the TC3_MNE path. At the landfall location, the peak period of the positive surge can be deferred from that of the baseline as the mean sea
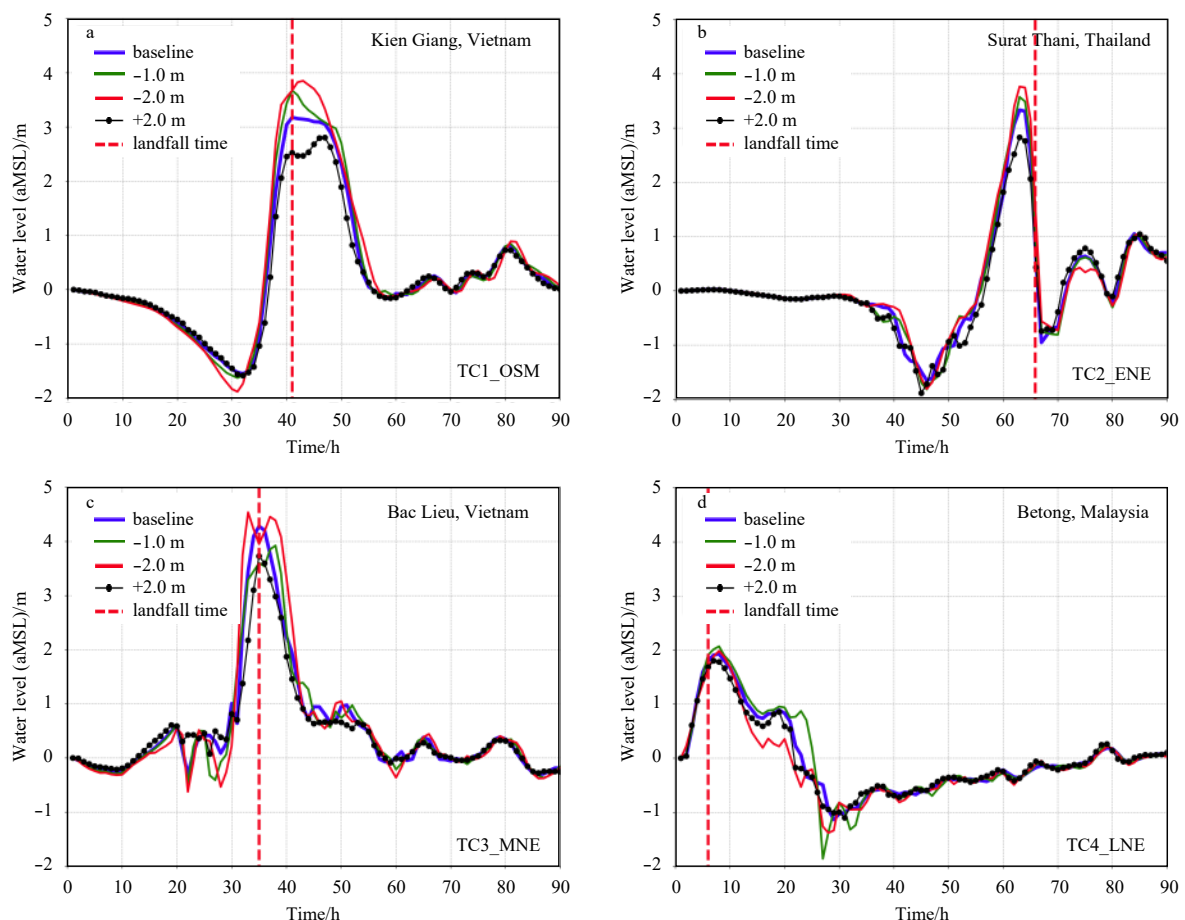

Fig. 7. Intensification of storm surges in some particular regions influenced by hypothetical tropical cyclones and mean sea level (MSL) conditions. Dash line indicates the time when storms make the shortest distance from the coast.

level becomes shallower (Fig. 5c, black dots, solid curve). At the inner GOT where the topographic factor is lesser, such behavior is even more pronounced (Fig. 6c, green and red curves). On the other hand, the shallower sea level tends to accelerate the time to peak of the minimum surge (Fig. 5c, blue dots, solid curve). This behavior is also seen in the result of the TC4_LNE path (Fig. 5d, blue dots, solid curve). However, the overall rhythmic structures are unchanged.

The periods of the oscillation for the surges above are approximately 25 hours (peak-to-peak). This characteristic suggests that sea level variability has an insignificant impact on the temporal structure of storm surges in the gulf. This also indicates that the resonance modal structures should remain unchanged. The delayed surge, however, seems to be more amplified but it does not conform to the resonance response of the gulf (Tomkratoke et al., 2015) and that of the SCS (Chen et al., 2012). Other mechanisms such as an interaction between surge and shelf bathymetry may help explain this phenomenon. The details of this interaction are presented next.

3.4.2 *Shelf bathymetry*

As presented in Fig. 5–7, the storm surge magnitude tends to be more amplified or weaken as the mean sea level decreases or increases, respectively. This conforms to the nonlinear effect revealed by Horsburgh and Wilson (2007) and Rego and Li (2010) who reported that high surges did not occur at high water depths. However, the development of a high surge in the GOT-SS has a unique mechanism because of the high complexity of hydrodynamic processes. Here, the funnel-shaped or concave shoreline indeed promotes amplification of the surges as described in Section 3.2. Even in the near landfall location, the storm surge response at the long straight coastline (Prachuap Khiri Khan, Thailand) increases, but not as much as found at the concave coastline (Bac Lieu, Vietnam) and the funnel-shaped bays (Kien Giang, Vietnam; Surat Thani and Samut Prakan, Thailand; Betong, Malaysia) (Figs 4 and 7). In comparison, the increment of surge magnitude in the latter regions can exceed 0.5 times the baseline case while the surge magnitude at the straight coastline is much lower.

To explain the mechanism of amplification, the vertical structure of the current need to be interpreted. This interpretation can help one examine how the storm surge flow structure evolves under various mean sea level conditions. In doing so, deviation of surface and bottom currents and surge magnitude between the scenarios and baseline for only the two upper paths (TC1_OSM and TC2_ENE) are determined and presented in Fig. 8. Suggested by the maximum storm surge magnitude results (Fig. 4), the most hazard prone region for the TC1_OSM path is the inner GOT while the Surat Thani and Bac Lieu are the most hazard prone areas for the TC2_ENE path. For the current structure in those regions, both surface and bottom, larger deviations are seen in the –2.0 meters scenario, especially, in the nearshore region (Fig. 8, upper panel). Hence, the induced currents are stronger than that of the baseline. This scenario also produces larger deviations in surge magnitude. In contrast, a minor deviation is observed in the high-water scenario (Fig. 8, lower panel).

From the response behavior and relationships between the current structure and surge levels in nearshore regions, it is found that the amplification of storm surges is proportional to the flow strength and tends to be more intensified in regions with a funnel or concave shaped coastline. The amplification conforms well to the importance of shelf bathymetry on coastal

surges which can be illustrated as (Pugh, 1987): $\eta \propto \dfrac{LCW^2}{H}$. Where η is the surge height, L is the shelf width, H is the total water depth. W is the wind speed and C is a constant combining gravity, density and empirical drag.

Because of the wind stress become more effective in shallow water, the water surface can be significantly raised and bottom stress increases. Enhancement of the current through the vertical axis also relies on the mass continuity principle where the flow speed increases with decreasing cross-sectional area. Hence, regardless of the shallow bathymetry, the funnel effect also induces greater intensification of storm surges in the nearshore region of the GOT-SS. Small amplification in the offshore sector is normally due to a reduction of damping or bottom friction in deeper sea.

In summary, we have investigated four factors: phase propagation of the storm surge wave determined by the landfall position, the funnel effect caused by locality of the coastline, shelf bathymetry determined by the state of mean sea level and the coastline crossing angle of the storm path. By identifying the important physical mechanisms that induce severe surges, we found that the induced surge in particular regions can be regarded as significantly high.

4 Conclusions

In the present study, the influence of tropical cyclone paths and shelf bathymetry on the inducement of severe storm surges in the Gulf of Thailand-Sunda Shelf is determined via numerical hydrodynamic simulations and a parametric wind model.Our validation study shows good agreement between a simulated and observed storm surge. The contributions of each significant factor on the generation of severe surges in the region are summarized as follows:

Storm paths can play a substantial role in controlling oscillation patterns of storm surges in the gulf. Tropical cyclones moving along a monsoon trough during the onset to early northeast monsoon season (October-November, TC1_OSM and TC2_ENE scenarios, passing over the upper part of the gulf) produce a signature mirrored N-shaped surge. In contrast, tropical cyclones in the mid and late northeast monsoon season (December-January, TC3_MNE and TC4_LNE, passing over the lower part of the gulf) mainly induce a single flood surge. Supported by the flood surge period, the funnel effect, and the effective angle of crossing, a severe surge can be induced in particular regions of the Gulf of Thailand-Sunda Shelf, especially in regions with monsoon trough development during the onset to early northeast monsoon season.

Varying depth (mean sea level) does not show a significant contribution to the temporal and resonance modal structures of storm surges in the gulf. Instead, a significant surge amplification occurs. This amplification is inversely pronounced as depth increases, and it conforms well with the importance of shelf bathymetry on coastal surges as theorized by Pugh (1987). However, as suggested by the flow structure, the amplification in particular regions may be simply explained based on continuity of mass.

Given that the GOT consists of complicated geomorphic structures that can amplify storm surge magnitudes as revealed in the current study, the precise forecast of storm paths must be incorporated in developing oceanic disaster forecasting systems.

Finally, the highlights of this study are: this study is first to provide the key mechanisms of tropical cyclone paths and shelf bathymetry on the inducement of severe storm surges in the Gulf
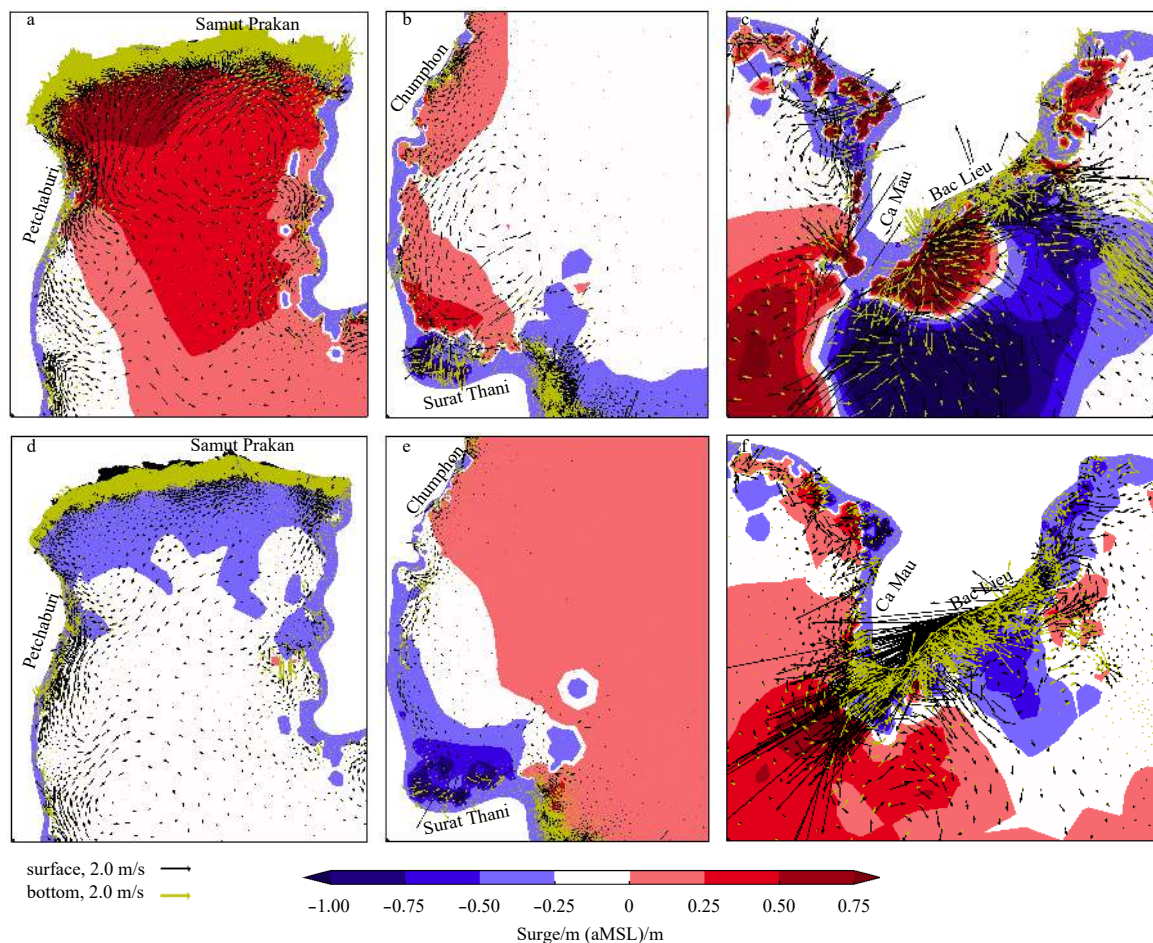
Fig. 8. Current magnitude (arrows) and surge level (filled contour) deviations of scenario mean sea levels (upper: baseline –2.0 m and lower: baseline +2.0 m), at the highest surge regions i.e. the inner GOT (a and b, TC1_OSM), Surat Thani Bay (c and d, TC2_ENE) and Ca Mau peninsula (e and f, TC2_ENE).

of Thailand-Sunda Shelf. This study also provides the important foundation information extreme surges in developing oceanic disaster forecasting systems as well as storm surge preparedness and safety for the Gulf of Thailand-Sunda Shelf. And, this study can be also used as the guidance and support for field surveys studies of storm surge disasters in the Gulf of Thailand-Sunda Shelf.

References

Aschariyaphotha N, Wongwises P, Humphries U W, et al. 2011. Study of storm surge due to Typhoon Linda (1997) in the Gulf of Thailand using a three dimensional ocean model. Applied Mathematics and Computation, 217(21): 8640–8654, doi: 10.1016/j.amc.2011.03.105

As-Salek J A. 1998. Coastal trapping and funneling effects on storm surges in the Meghna Estuary in relation to cyclones hitting Noakhali–Cox's Bazar Coast of Bangladesh. Journal of Physical Oceanography, 28(2): 227–249, doi: 10.1175/1520-0485(1998)028<0227:CTAFEO>2.0.CO;2

Cavaleri L, Sclavo M. 2006. The calibration of wind and wave model data in the Mediterranean Sea. Coastal Engineering, 53(7): 613–627, doi: 10.1016/j.coastaleng.2005.12.006

Chen Changsheng, Liu Hedong, Beardsley R C. 2003. An unstructured grid, finite-volume, three-dimensional, primitive equations ocean model: application to coastal ocean and estuaries. Journal of Atmospheric and Oceanic Technology, 20(1): 159–186, doi: 10.1175/1520-0426(2003)020<0159:AUGFVT>2.0.CO;2

Chen C, Beardsley R C, Cowles G. 2006. An unstructured grid, finite-volume coastal ocean model (FVCOM) system. Oceanography, 19(1): 78–89, doi: 10.5670/oceanog.2006.92

Chen Haoliang, Tkalich P, Malanotte-Rizzoli P, et al. 2012. The forced and free response of the South China Sea to the large-scale monsoon system. Ocean Dynamics, 62(3): 377–393, doi: 10.1007/s10236-011-0511-7

Debsarma S K. 2009. Simulations of storm surges in the Bay of Bengal. Marine Geodesy, 32(2): 178–198, doi: 10.1080/01490410902869458

Digital Typhoon. 2016. Typhoon 199726 (LINDA)-General Information (Pressure and Track Charts). http://agora.ex.nii.ac.jp/digital-typhoon/summary/wnp/s/199726.html.en [2016-05-05]

Flather R A. 1994. A storm surge prediction model for the northern Bay of Bengal with application to the cyclone disaster in April 1991. Journal of Physical Oceanography, 24(1): 172–190, doi: 10.1175/1520-0485(1994)024<0172:ASSPMF>2.0.CO;2

Holland G J. 1980. An analytic model of the wind and pressure profiles in hurricanes. Monthly Weather Review, 108(8): 1212–1218, doi: 10.1175/1520-0493(1980)108<1212:AAMOTW>2.0.CO;2

Horsburgh K J, Wilson C. 2007. Tide-surge interaction and its role in the distribution of surge residuals in the North Sea. Journal of Geophysical Research, 112(C8): C08003

Hussain M A, Tajima Y. 2017. Numerical investigation of surge–tide interactions in the Bay of Bengal along the Bangladesh coast. Natural Hazards, 86(2): 669–694, doi: 10.1007/s11069-016-2711-4

IOC, IHO and BODC. 2003. "Centenary Edition of the GEBCO Digital Atlas", published on CD-ROM on behalf of the Intergovernmental Oceanographic Commission and the International Hydrographic Organization as part of the General Bathymetric Chart of the Oceans; British Oceanographic Data Centre, Liverpool

Jelesnianski C P. 1965. A numerical calculation of storm tides induced by a tropical storm impinging on a continental shelf. Monthly Weather Review, 93(6): 343–358, doi: 10.1175/1520-0493(1993)093<0343:ANCOS>2.3.CO;2

Kanbua W, Supharatid S, Tang I M. 2005. Ocean wave forecasting in the gulf of Thailand during typhoon Linda 1997: WAM and Neural network approaches. ScienceAsia, 31(3): 243–250, doi: 10.2306/scienceasia1513-1874.2005.31.243

Kohno N, Kamakura K, Minematsu H, et al. 2007. The mechanism of the storm surges in the Seto inland sea caused by Typhoon Chaba (0416). Technical Review 9. RSMC Tokyo-Typhoon Center

Lander M A. 1996. Specific tropical cyclone track types and unusual tropical cyclone motions associated with a reverse-oriented monsoon trough in the western North Pacific. Weather and Forecasting, 11(2): 170–186, doi: 10.1175/1520-0434(1996)011<0170:STCTTA>2.0.CO;2

Pan Yi, Chen Yongping, Li Jiangxia, et al. 2016. Improvement of wind field hindcasts for tropical cyclones. Water Science and Engineering, 9(1): 58–66, doi: 10.1016/j.wse.2016.02.002

Phaksopa J, Sojisuporn P. 2006. Storm surge in the Gulf of Thailand generated by typhoon Linda in 1997 using Princeton Ocean Model (POM). Kasetsart Journal (Natural Science), 40(5): 260–268

Proudman J. 1955. The propagation of tide and surge in an estuary. Proceedings of the Royal Society A: Mathematical, Physical and Engineering Sciences, 231(1184): 8–24

Pugh D T. 1987. Tides, Surges, and Mean Sea-Level: A Handbook for Engineers and Scientists. Chichester: John Wiley and Sons

Rego J L, Li Chunyan. 2010. Nonlinear terms in storm surge predictions: effect of tide and shelf geometry with case study from Hurricane Rita. Journal of Geophysical Research, 115(C6): C06020

Saramul S. 2017. Seasonal monsoon variations in surface currents in the Gulf of Thailand revealed by high frequency radar. Engineering Journal, 21(4): 25–37, doi: 10.4186/ej.2017.21.4.25

Signell R P, Carniel S, Cavaleri L, et al. 2005. Assessment of wind quality for oceanographic modelling in semi-enclosed basins. Journal of Marine Systems, 53(1–4): 217–233

Sirisup S, Kitamoto A. 2012. An unstructured normal mode decomposition solver on real ocean topography for the analysis of storm tide hazard. In: Proceedings of 2012 Oceans-Yeosu. Yeosu, South Korea: IEEE, 1–7

Takahashi H G, Fujinami H, Yasunari T, et al. 2015. Role of tropical cyclones along the monsoon trough in the 2011 Thai flood and interannual variability. Journal of Climate, 28(4): 1465–1476, doi: 10.1175/JCLI-D-14-00147.1

Terry J P, Jankaew K, Dunne J. 2015. Coastal vulnerability to typhoon inundation in the Bay of Bangkok, Thailand? Evidence from carbonate boulder deposits on Ko Larn island. Estuarine, Coastal and Shelf Science, 165: 261–269, doi: 10.1016/j.ecss.2015.05.028

Tomkratoke S, Sirisup S, Udomchoke V, et al. 2015. Influence of resonance on tide and storm surge in the Gulf of Thailand. Continental Shelf Research, 109: 112–126, doi: 10.1016/j.csr.2015.09.006

Vongvisessomjai S. 2007. Impacts of typhoon Vae and Linda on wind waves in the upper gulf of Thailand and East Coast. Songklanakarin Journal of Science and Technology, 29(5): 1199–1216

Williams H, Choowong M, Phantuwongraj S, et al. 2016. Geologic records of Holocene typhoon strikes on the Gulf of Thailand coast. Marine Geology, 372: 66–78, doi: 10.1016/j.margeo.2015.12.014

Wu Liang, Wen Zhiping, Huang Ronghui, et al. 2012. Possible linkage between the monsoon trough variability and the tropical cyclone activity over the western North Pacific. Monthly Weather Review, 140(1): 140–150, doi: 10.1175/MWR-D-11-00078.1

Zu Tingting, Gan Jianping, Erofeeva S Y. 2008. Numerical study of the tide and tidal dynamics in the South China Sea. Deep Sea Research Part I: Oceanographic Research Papers, 55(2): 137–154, doi: 10.1016/j.dsr.2007.10.007